

NOTES ON PLANE PARTITIONS

1. BASICS OF PARTITIONS

Let n be a positive integer. An *integer partition* of n (often just called a partition of n) is a way to write n as a sum of non-negative integers. For example, one partition of $n = 3$ is $3 = 2 + 1$. We do not distinguish between different rearrangements of the summands, that is, we treat $2 + 1$ and $1 + 2$ as the same partition. If λ is a partition of n , we usually write it as a tuple of the summands put in decreasing order:

$$\lambda = (\lambda_1, \lambda_2, \dots, \lambda_k)$$

with $\lambda_1 \geq \lambda_2 \geq \dots \geq \lambda_k > 0$ and $\lambda_1 + \dots + \lambda_k = n$. Each summand is called a *part* of the partition. For example, λ_1 is the first part and λ_i is the i th part. The total number of parts of a partition is called its *length* and is written $\ell(\lambda)$.

Example 1.1. Let $n = 3$. There are 3 different partitions of $n = 3$. We have

$$(3), \quad (2, 1), \quad \text{and} \quad (1, 1, 1).$$

We have $\ell((3)) = 1$, $\ell((2, 1)) = 2$, and $\ell((1, 1, 1)) = 3$.

Remark 1.2. It will sometimes be convenient to add extra parts equal to zero to the end of our partitions, sometimes infinitely many of them. You may see partitions given as

$$\lambda = (\lambda_1, \lambda_2, \lambda_3, \dots)$$

with $\lambda_1 \geq \lambda_2 \geq \lambda_3 \geq \dots \geq 0$. In this case, the length of a partition is the number of nonzero parts.

Exercise 1. List all partitions of 5 as well as their lengths. (Difficulty rating: 1)

Let $p(n)$ be the number of partitions of n . For $n = 0, 1, 2, 3, 4, 5$ we have

$$p(n) = 1, 1, 2, 3, 5, 7$$

respectively. (By convention we have $p(0) = 1$ as only the empty sum sums to zero.) The *generating function* of p is the infinite series

$$\sum_{n=0}^{\infty} p(n)q^n = 1 + q + 2q^2 + 3q^3 + 5q^4 + 7q^5 + \dots$$

There is no known closed formula for the sum, but it can be expressed as an infinite product.

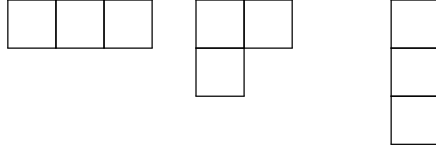
Theorem 1.3. We have

$$\sum_{n=0}^{\infty} p(n)q^n = \prod_{j=1}^{\infty} \frac{1}{1 - q^j}$$

where this is an equality of power series (one should think of each term in the product on the RHS as a geometric series $\frac{1}{1-r} = 1 + r + r^2 + \dots$).

We will often depict partitions pictorially in the form of *Young diagrams*. These are collections of boxes such that the number of boxes in the i th row is equal to the i th part of the partition. It is easiest to see in an example.

Example 1.4. For the partitions of 3, the Young diagrams are

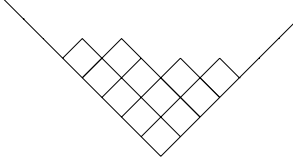


$$\lambda = (3) \quad \lambda = (2, 1) \quad \lambda = (1, 1, 1)$$

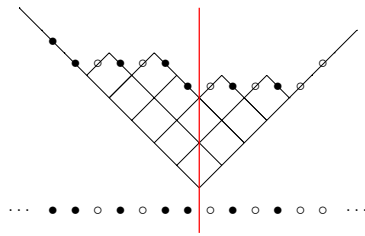
Note that we are drawing the largest part as the top row. This is the *English convention*. The *French convention* has the largest part on bottom and the smallest on top.

Exercise 2. Draw the Young diagram for each partition you found in Exercise 1. (Difficulty rating: 1)

It will be useful for us in what follows to have another perspective through which we can view partitions. Consider the Young diagram of a partition λ drawn in *Russian convention* (French convention rotated 45° counter-clockwise). For example, if $\lambda = (4, 3, 2, 2, 1)$ we draw



The boundary of the partition then becomes a path with steps of the form $(1, 1)$ and $(1, -1)$. Assign to each $(1, -1)$ step a particle (or filled dot) and to each $(1, 1)$ step a hole (or unfilled dot). Project this sequence of particles and holes to the horizontal axis, and extend it infinitely to the left with particles and infinitely to the right with holes. This sequence of particles and holes is known as the *Maya diagram* of the partition. In our example, we have



Note there is a unique point where the number of particles to the right of that point is equal to the number of holes to the left. We call this *center* of the Maya diagram and draw it in red in the above. We will think of the center being at 0 and the particles as being on the half-integers. In the example above the particle position, starting with the right-most, are given by

$$(3.5, 1.5, -0.5, -1.5, -3.5, -5.5, -6.5, \dots)$$

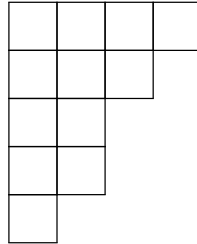
In fact, if $\lambda = (\lambda_1, \lambda_2, \dots)$, including infinitely many zero parts, then the particles are at positions $\lambda_i - i + \frac{1}{2}$ for $i = 1, 2, \dots$

While we consider Maya diagrams as bi-infinite sequences of particles and holes, notice that for any given partition λ there is only a finite interval in which anything “interesting” happens. If λ_1 is the length of the first row of λ and λ'_1 the length of the first column, then the right-most particle is at $\lambda_1 - \frac{1}{2}$ and the left-most hole is at $-\lambda'_1 + \frac{1}{2}$.

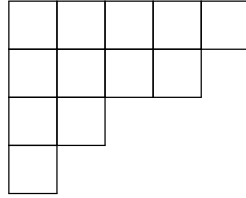
Exercise 3. Draw the Maya diagram for each partition you found in Exercise 1. (Difficulty rating: 1)

The *conjugate partition* of a partition λ is the partition you get by reflecting the Young diagram of λ over its main diagonal. We denote it λ' .

Example 1.5. Consider the partition $\lambda = (4, 3, 2, 2, 1)$. Its Young diagram is given by



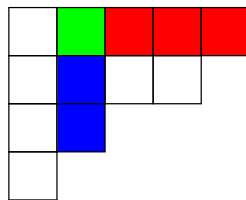
Reflecting this around the main diagonal gives



We see that $\lambda' = (5, 4, 2, 1)$.

We will often identify a partition λ with its Young diagram and write $x \in \lambda$ to mean a specific square (or *cell*) x in the Young diagram. For a cell $x \in \lambda$ we define the *arm* of x to be the cells to the right of x in the same row and we denote the number of such cells $\text{arm}_\lambda(x)$. Similarly, we define the *leg* of x to be the cells below x in the same column and denote the number of such cells $\text{leg}_\lambda(x)$. The *hook* of the cell x is all the cells in its arm and its leg as well as the cell itself. The number of cells in the hook of x is called the *hook length* and is denoted $h_\lambda(x)$. Note that $h_\lambda(x) = \text{arm}_\lambda(x) + \text{leg}_\lambda(x) + 1$.

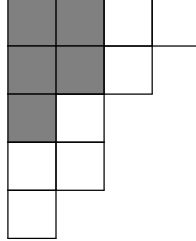
Example 1.6. Consider the cell x , marked in green, in the partition $\lambda = (5, 4, 2, 1)$. We color the cells in its arm red and those in its leg blue.



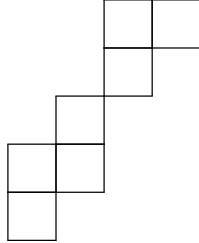
We have $\text{arm}_\lambda(x) = 3$, $\text{leg}_\lambda(x) = 2$ and $h_\lambda(x) = 6$.

If we have two partitions μ and λ we say that μ is *contained* in λ and write $\mu \subseteq \lambda$ if the Young diagram for μ is contained in the Young diagram for λ . When $\mu \subseteq \lambda$ we define the *skew diagram* λ/μ to be the set of cells in the Young diagram for λ that are not in the Young diagram for μ . λ/μ is called a *skew partition*. Skew things are not so important for these notes, but much of what we do in what follows can be extended to the skew case.

Example 1.7. Consider the partitions $\mu = (2, 2, 1)$ and $\lambda = (4, 3, 2, 2, 1)$. We draw the two Young diagram below with the gray squares indicating the diagram for μ .



The skew diagram for the skew partition $\lambda/\mu = (4, 3, 2, 2, 1)/(2, 2, 1)$ is given by



2. INTERLACING PARTITIONS

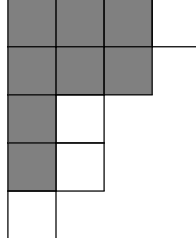
We say that two partitions μ and λ *interlace* if

$$\lambda_1 \geq \mu_1 \geq \lambda_2 \geq \mu_2 \geq \dots$$

and write $\mu \preceq \lambda$. Equivalently, $\mu \preceq \lambda$ if and only if one can get the Young diagram of λ from the Young diagram of μ by adding at most one cell to each column. We say that the two partitions differ by a *horizontal strip*. Note that for μ and λ to interlace we necessarily have $\mu \subseteq \lambda$.

We say that μ and λ *co-interlace* if their conjugate partitions interlace, that is, $\mu' \preceq \lambda'$. We write $\mu \preceq' \lambda$. Note one can get the Young diagram of λ from the Young diagram of μ by adding at most one cell to each row. We say that the two partitions differ by a *vertical strip*.

Example 2.1. The partitions $\mu = (3, 3, 1, 1)$ and $\lambda = (4, 3, 2, 2, 1)$ satisfy $\mu \preceq' \lambda$ since we can get λ from μ by adding at most one cell to each row. Below we draw the Young diagram of μ in gray and the vertical strip you need to add to get λ in white.



Note that these partitions do not satisfy $\mu \preceq \lambda$ since we need to add two cells to the second column of μ to get λ .

Many different objects in combinatorics can be shown to be in bijection with sequences of (co-)interlacing partitions. The study of the probabilistic aspects of such sequences of partitions is known as the study of *Schur processes*. We'll mostly stick to the combinatorics and look at only a few examples.

2.1. Semi-standard Young tableaux. A semi-standard Young tableaux of shape λ is a filling of the cells of the Young diagram of λ by entries in $\{1, 2, \dots, n\}$ such that:

- The entries are weakly increasing across the rows.
- The entries are strictly increasing down the columns.

Proposition 2.2. *There is a bijection between semi-standard Young tableaux of shape λ with entries in $\{1, 2, \dots, n\}$ and sequence of partitions*

$$\emptyset = \lambda^{(0)} \preceq \lambda^{(1)} \preceq \dots \preceq \lambda^{(n-1)} \preceq \lambda^{(n)} = \lambda$$

The idea of the proof is that $\lambda^{(i)}$ is the partition you get by looking at all the cells with filling $\leq i$. It is best seen via an example.

Example 2.3. An example of a SSYT of shape $\lambda = (4, 3, 1)$ filled with entries in $\{1, 2, 3, 4\}$.

<table border="1" style="border-collapse: collapse; width: 100%; height: 100%;"> <tr><td>1</td><td>1</td><td>2</td><td>4</td></tr> <tr><td>2</td><td>2</td><td>3</td><td></td></tr> <tr><td>4</td><td></td><td></td><td></td></tr> </table>	1	1	2	4	2	2	3		4				<table border="1" style="border-collapse: collapse; width: 100%; height: 100%;"> <tr><td>1</td><td>1</td><td></td><td></td></tr> <tr><td></td><td></td><td></td><td></td></tr> <tr><td></td><td></td><td></td><td></td></tr> </table>	1	1											<table border="1" style="border-collapse: collapse; width: 100%; height: 100%;"> <tr><td></td><td></td><td>2</td><td></td></tr> <tr><td></td><td></td><td></td><td></td></tr> <tr><td></td><td></td><td></td><td></td></tr> </table>			2										<table border="1" style="border-collapse: collapse; width: 100%; height: 100%;"> <tr><td></td><td></td><td></td><td></td></tr> <tr><td></td><td></td><td></td><td></td></tr> <tr><td></td><td></td><td></td><td></td></tr> </table>													<table border="1" style="border-collapse: collapse; width: 100%; height: 100%;"> <tr><td></td><td></td><td></td><td></td></tr> <tr><td></td><td></td><td></td><td></td></tr> <tr><td></td><td></td><td></td><td></td></tr> </table>												
1	1	2	4																																																													
2	2	3																																																														
4																																																																
1	1																																																															
		2																																																														
	$\lambda^{(1)} = (2)$	$\lambda^{(2)} = (3, 2)$	$\lambda^{(3)} = (3, 3)$	$\lambda^{(4)} = (4, 3, 1)$																																																												

We also list the corresponding sequence of interlacing partitions.

We can write down a generating function for these tableaux. Assign to each tableaux T a monomial in the variables x_1, x_2, \dots, x_n given by

$$x^T = x_1^{\# \text{ of } 1\text{'s}} x_2^{\# \text{ of } 2\text{'s}} \dots x_n^{\# \text{ of } n\text{'s}}$$

We can then write down a polynomial

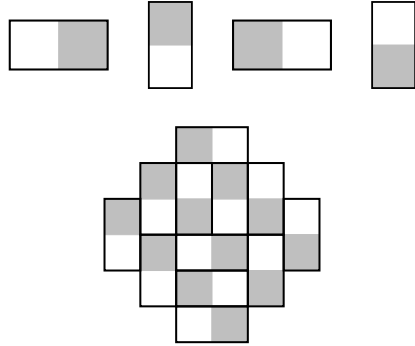
$$s_\lambda(x_1, \dots, x_n) = \sum_{T \in \text{SSYT}(\lambda)} x^T$$

where the sum is over all semi-standard Young tableaux of shape λ with entries in $\{1, 2, \dots, n\}$. This is known as a *Schur polynomial*. These polynomials are ubiquitous in combinatorics and also make appearances representation theory, probability, and mathematical physics.

Exercise 4. List all SSYT with shape $\lambda = (3, 2, 1)$ with entries in $\{1, 2, 3\}$. (Difficulty rating: 1)

Exercise 5. Prove Proposition 2.2. (Difficulty rating: 2)

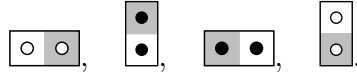
2.2. Tilings of the Aztec diamond. Let A_{N+1} be the union of faces of \mathbb{Z}^2 which are entirely contained in the region $|x| + |y| \leq N+1$. A tiling of the Aztec diamond of rank N is a tiling of the region A_{N+1} with 2×1 or 1×2 dominos. The four possible dominos and an example of a tiling of the Aztec diamond of rank 3 are shown below:



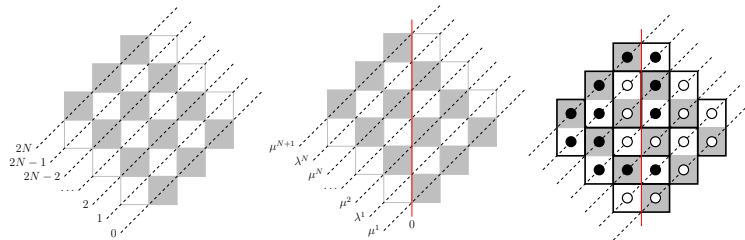
Proposition 2.4. *There is a bijection between tilings of the Aztec diamond of rank N and sequences of interlacing partitions*

$$\emptyset = \mu^{(1)} \preceq \lambda^{(1)} \succeq' \mu^{(2)} \preceq \dots \preceq \lambda^{(N-1)} \succeq' \mu^{(N)} \preceq \lambda^{(N)} \succeq' \mu^{(N+1)} = \emptyset.$$

To prove this we turn to the Maya diagrams. Given a tiling of the Aztec diamond of rank N assign particles and holes to the dominos according to the rules



Along each diagonal slice of the Aztec diamond view the resulting sequence of particles and holes as the Maya diagram of some partition by extending it infinitely to the South-West with particles and infinitely to the North-East by holes. Let us index the slices starting from 0, such that $\mu^{(i)}$ is the partition along slice $2i - 2$ and $\lambda^{(i)}$ is the partition along slice $2i - 1$. Note that $\mu^{(1)} = \mu^{(N+1)} = \emptyset$ is forced. We give an example below. The center of the Maya diagrams is marked in red.



The example tiling on the left above corresponds to the sequence of partitions

$$\begin{aligned} \mu^{(1)} &= \emptyset, & \lambda^{(1)} &= (1) \\ \mu^{(2)} &= \emptyset, & \lambda^{(2)} &= (1, 0) \\ \mu^{(3)} &= (1, 0), & \lambda^{(3)} &= (1, 0, 0) \\ \mu^{(4)} &= \emptyset \end{aligned}$$

Exercise 6. List all 8 tilings of the Aztec diamond of rank 2 and the corresponding sequence of partitions. (Difficulty rating: 1)

Exercise 7. Construct the tiling that corresponds to the sequence of partitions:

$$\begin{aligned}\mu^{(1)} &= \emptyset, & \lambda^{(1)} &= (2) \\ \mu^{(2)} &= (2), & \lambda^{(1)} &= (2, 1) \\ \mu^{(3)} &= (1, 0), & \lambda^{(3)} &= (1, 1, 0) \\ \mu^{(4)} &= \emptyset\end{aligned}$$

(Difficulty rating: 1)

Exercise 8. Prove Proposition 2.4. (Difficulty rating: 3)

Exercise 9. Note that for tilings of the Aztec diamond we alternate between \preceq and \succeq' . What sort of tilings do we get if you we use a different sequence of interlacing conditions? That is, we choose some element $I \in \{\preceq, \succeq'\}^{2n}$, look at sequences of interlacing partitions

$$\emptyset = \lambda^{(1)} I_1 \lambda^{(2)} I_2 \dots \lambda^{(2n)} I_{2n} \lambda^{(2n+1)} = \emptyset,$$

and determine what sort of domino tilings this is in bijection with. The resulting tilings are known as steep tilings. (Difficulty rating: 3)

3. PLANE PARTITIONS

Plane partitions are the two-dimensional analogue of integer partitions. We can define *plane partitions* as arrays of non-negative integers that are weakly decreasing along the rows and also weakly decreasing down the columns. Note that we allow filling by zero. Sometimes we will restrict the number of rows or columns the plane partition is allowed to have, but otherwise we consider bi-infinite arrays. The *volume* of a plane partition is the sum of all the entries in the plane partition.

Example 3.1. A possible plane partition restricted to 3 rows and 4 columns:

6	6	3	3
4	3	3	0
2	2	0	0

It has volume 32.

The following theorem gives the generating function of the plane partitions.

Theorem 3.2. Let $pp(n)$ be the number of plane partitions with volume n . The generating function for the number of plane partitions is

$$\sum_{\Lambda, P.P.} q^{|\Lambda|} = \sum_{n=0}^{\infty} pp(n)q^n = \prod_{n=1}^{\infty} \frac{1}{(1-q^n)^n}$$

for $|q| < 1$.

Exercise 10. By expanding the RHS of the generating function in Thm. 3.2 as a power series in q , determine the number of plane partitions of volume 3. List them. (Difficulty rating: 1)

If we fix the number of rows to be k and the length of each row to be r , then the number of such plane partitions also has a nice product formula.

Proposition 3.3. *Fix the number of rows to be k and the length of each row to be r . The number of such plane partitions is given by*

$$\sum_{\Lambda, \text{ P.P. with } k \text{ rows and } r \text{ cols}} q^{|\Lambda|} = \prod_{i=1}^r \prod_{j=1}^k \frac{1}{1 - q^{i+j-1}}$$

Exercise 11. Prove Thm. 1.3 starting from Prop. 3.3. (Difficulty rating: 2)

3.1. Reverse Plane partitions. A *reverse plane partition* is what you get when you rotate the plane partition by 180 degrees. Equivalently, you think of filling the rows and columns with weakly increasing non-negative integers. For example:

6	6	3	3
4	3	3	0
2	2	0	0

↔

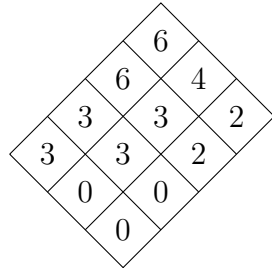
0	0	2	2
0	3	3	4
3	3	6	6

We can fix the length of each row by giving the reverse plane partition a shape: a *reverse plane partition of shape λ* is a filling of the Young diagram of λ by non-negative integers that are weakly increasing along the rows and columns. For example, let $\lambda = (4, 3, 1)$, then one possible reverse plane partition of shape λ is

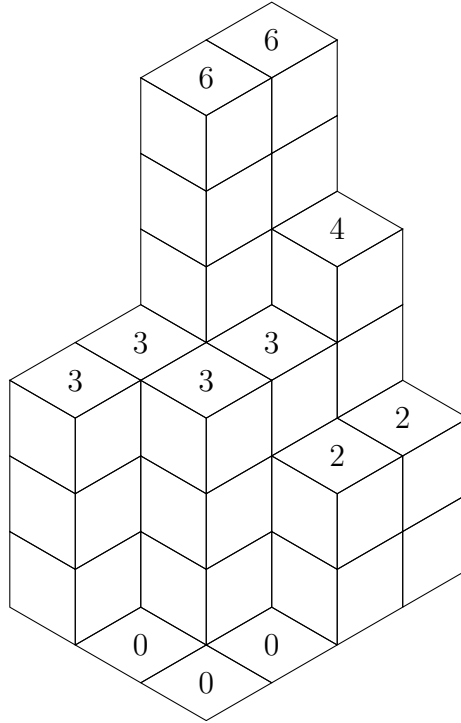
0	0	2	3
1	2	4	
1			

One way to visualize reverse plane partitions is as stacks of cubes where the filling tells you the height of the column of cubes.

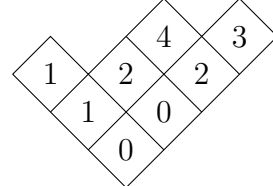
Example 3.4. Consider the RPP of shape $\lambda = (4, 4, 4)$ drawn in Russian convention below



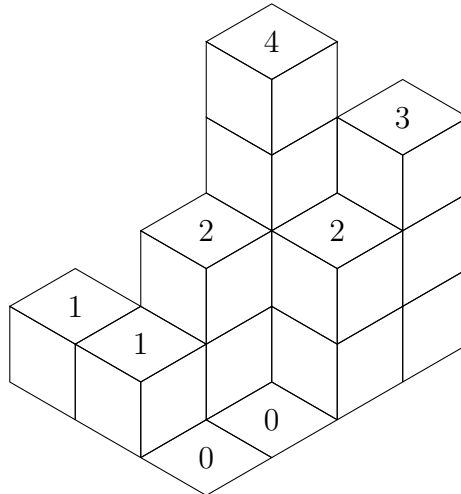
We can draw it as a stack of cubes



Similarly, the RPP of shape $\lambda = (4, 3, 1)$ given above takes the form

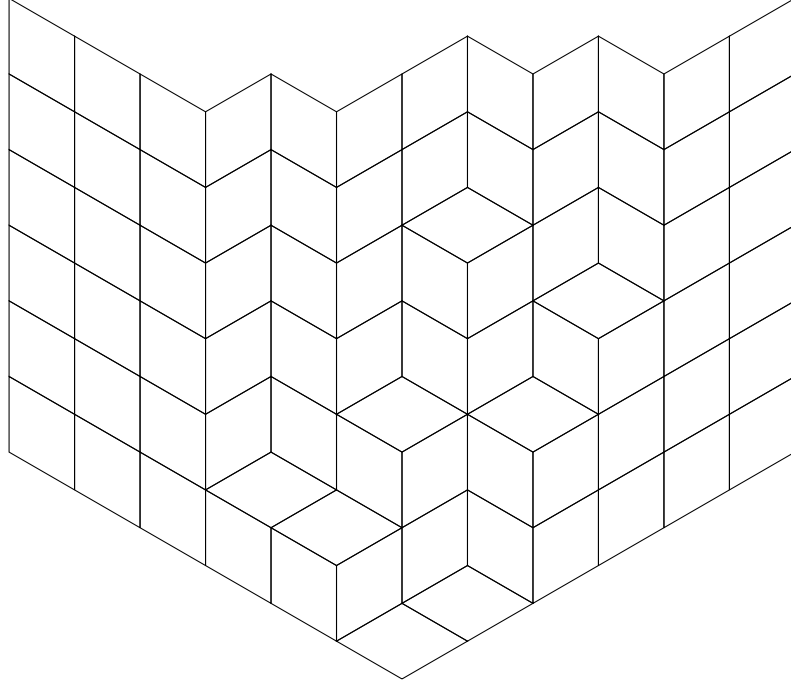


in Russian convention. The corresponding stack of cubes is



Remark 3.5. Rather than stacks of cubes, one may instead view the RPP as a tiling of the upper third of the plane by rhombuses (also known as a lozenge tiling). For

example, the same RPP of shape $(4, 3, 1)$ could be drawn as the tiling



where the pattern continues infinitely to right, left, and upward.

Clearly, the generating function for reverse plane partitions of shape

$$\lambda = \underbrace{(r, \dots, r)}_{k \text{ times}}$$

is given by the formula in Prop. 3.3. But we can do better.

Theorem 3.6. Let $RPP(\lambda)$ be the set of all reverse plane partitions of shape λ . We have

$$\sum_{\Lambda \in RPP(\lambda)} q^{|\Lambda|} = \prod_{x \in \lambda} \frac{1}{1 - q^{h_\lambda(x)}}$$

where the product is over all cells of the Young diagram of λ and $h_\lambda(x)$ is the hook length of the cell x in λ .

Example 3.7. Let $\lambda = (4, 3, 1)$. The hook length of the cells of λ are given below:

6	4	3	1
4	2	1	
1			

Theorem 3.6 says

$$\sum_{\Lambda \in RPP(\lambda)} q^{|\Lambda|} = \frac{1}{(1 - q^6)(1 - q^4)^2(1 - q^3)(1 - q^2)(1 - q)^3} = 1 + 3q + 7q^2 + \dots$$

Expanding this in power series, we see there is 1 reverse plane partitions of the given shape with volume 0, there are 3 with volume 1, there are 7 with volume 2 etc. We

list the seven with volume 2 below:

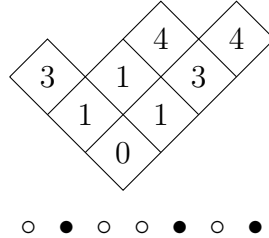
$\begin{array}{ c c c c } \hline 0 & 0 & 0 & 2 \\ \hline 0 & 0 & 0 & \\ \hline 0 & & & \\ \hline 0 & & & \\ \hline \end{array}$	$\begin{array}{ c c c c } \hline 0 & 0 & 0 & 0 \\ \hline 0 & 0 & 2 & \\ \hline 0 & 0 & 0 & \\ \hline 0 & & & \\ \hline \end{array}$	$\begin{array}{ c c c c } \hline 0 & 0 & 0 & 0 \\ \hline 0 & 0 & 0 & \\ \hline 2 & & & \\ \hline 0 & & & \\ \hline \end{array}$	$\begin{array}{ c c c c } \hline 0 & 0 & 0 & 1 \\ \hline 0 & 0 & 1 & \\ \hline 0 & & & \\ \hline 0 & & & \\ \hline \end{array}$	$\begin{array}{ c c c c } \hline 0 & 0 & 0 & 0 \\ \hline 0 & 1 & 1 & \\ \hline 0 & & & \\ \hline 0 & & & \\ \hline \end{array}$	$\begin{array}{ c c c c } \hline 0 & 0 & 0 & 1 \\ \hline 0 & 0 & 0 & \\ \hline 1 & & & \\ \hline 1 & & & \\ \hline \end{array}$	$\begin{array}{ c c c c } \hline 0 & 0 & 0 & 0 \\ \hline 0 & 0 & 1 & \\ \hline 1 & & & \\ \hline 1 & & & \\ \hline \end{array}$
---	---	---	---	---	---	---

Finally, we get to the bijection between reverse plane partitions of a fixed shape λ and certain sequences of partitions. This will be easiest to see in terms of an example.

Example 3.8. Consider the following reverse plane partition of shape $\lambda = (4, 3, 1)$:

0	1	3	4
1	1	4	
3			

We now draw it in Russian convention



○ ● ○ ○ ● ○ ○ ●

with the Maya diagram drawn below (only including from the left-most hole to the right-most particle). Set $\lambda^{(0)} = \lambda^{(7)} = \emptyset$. By reading the vertical slices from left to right we get a sequence of partitions $\lambda^{(1)}, \dots, \lambda^{(6)}$ given by

$$\begin{aligned} \lambda^{(1)} &= (3), & \lambda^{(2)} &= (1), & \lambda^{(3)} &= (1, 0), \\ \lambda^{(4)} &= (4, 1), & \lambda^{(5)} &= (3), & \lambda^{(6)} &= (4). \end{aligned}$$

where the partitions are determined by the filling on each vertical slice. These satisfy the interlacing conditions

$$\emptyset = \lambda^{(0)} \preceq \lambda^{(1)} \succeq \lambda^{(2)} \preceq \lambda^{(3)} \preceq \lambda^{(4)} \succeq \lambda^{(5)} \preceq \lambda^{(6)} \succeq \lambda^{(7)} = \emptyset$$

The interlacing conditions are determined by the shape λ . We see that we have a \preceq whenever the Maya diagram of λ has a hole and we have \succeq whenever the Maya diagram has a particle. That is, the sequence

○ ● ○ ○ ● ○ ○ ●

corresponds to the sequence of interlacing conditions

$$\preceq, \quad \succeq, \quad \preceq, \quad \preceq, \quad \succeq, \quad \preceq, \quad \succeq.$$

We state the following theorem that generalizes the above example.

Theorem 3.9. Let λ be a partition and set $n = h_\lambda((1, 1))$. There is a bijection between reverse plane partitions of shape λ and sequences of partitions $\lambda^{(0)}, \lambda^{(1)}, \dots, \lambda^{(n+1)}$ such that:

- $\lambda^{(0)} = \lambda^{(n+1)} = \emptyset$

- Suppose $I = (I_0, \dots, I_n) \in \{\preceq, \succeq\}^n$ is chosen such that $I_k = \preceq$ if there is a hole at $-\lambda'_1 + \frac{2k+1}{2}$ in the Maya diagram of λ and $I_k = \succeq$ otherwise. Then the sequence of partitions satisfy the interlacing condition

$$\emptyset = \lambda^{(0)} I_0 \lambda^{(1)} I_1 \lambda^{(2)} I_2 \dots I_n \lambda^{(n+1)} = \emptyset.$$

Exercise 12. Draw the reverse plane partition given in Example 3.8 as a rhombus tiling by viewing it in Russian convention and thinking of the filling in each cell as giving the height of a stack of cubes on that cell. (Difficulty rating: 1)

Exercise 13. Use Theorem 3.6 to give a formula for the generating function for reverse plane partitions of shape $(n, n-1, \dots, 2, 1)$. (Difficulty rating: 1)

Exercise 14. Prove Theorem 3.2 starting from Proposition 3.3 by taking the limit as $k, r \rightarrow \infty$. (Difficulty rating: 2)

Exercise 15. Prove Proposition 3.3 starting from Theorem 3.6. (Difficulty rating: 2)

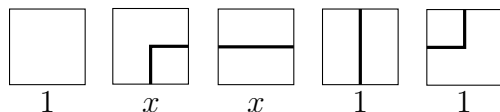
Exercise 16. Prove Theorem 3.9. (Difficulty rating: 2)

Note that if you have done all the exercises up to this point, then all that is left to prove is Thm. 3.6. We will do this in the Section 5 using vertex models.

4. FIVE-VERTEX MODELS

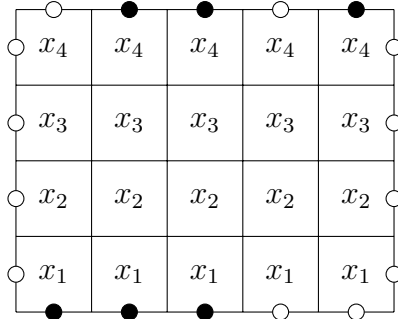
In this section we introduce *vertex models*. Vertex models encompass a large class of models originally arising in statistical physics, but now known to have deep connection to representation theory and, as we shall see, combinatorics. In broad strokes, consider the vertices $(i, j) \in \mathbb{Z}^2$. Suppose we have certain plaquettes we can place over each vertex and that there are restrictions on which plaquettes are allowed at neighboring vertices. Furthermore, we assign weights to the different plaquettes. The type of plaquettes along with the local restrictions and weights define the vertex model. While the above description is rather vague, it is in part because there are such a wide variety of vertex models that is hard to give a precise definition of what the term means. We would like to stress that the idea that we building blocks of our vertex model only “interact” locally in both the constraints and the weights. For our purposes it will be enough to focus on two types of five-vertex models, where “five” indicates the number of basic plaquettes.

4.1. The first five-vertex model. Now we describe the first five vertex model that will be of interest to us. The basic plaquettes are drawn below along with their corresponding weight:



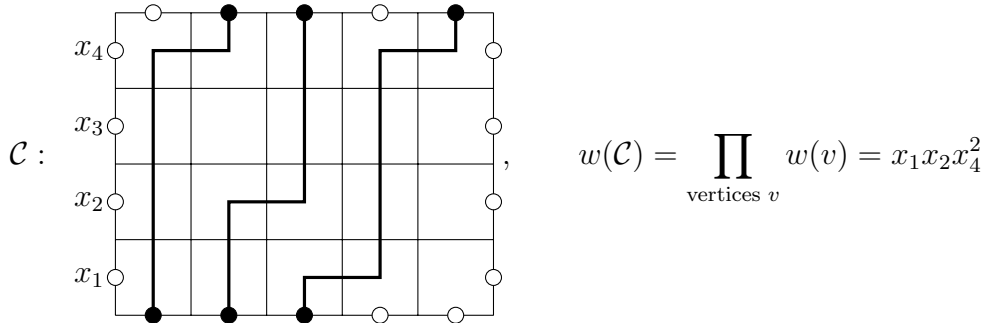
We think of each vertex as either being empty or having a path enter from the bottom or left and exit from the top or right. The local constraint on neighboring vertices is that the path segments must match up. We assign a weight of x whenever a path exits to the right. Note that it is not necessary for neighboring vertices to have the same weight parameter and often we will choose them to be different.

When considering a finite domain we have to impose *boundary conditions*, that is, rules for whether or not paths are entering or exiting the boundary of our domain. For example, we could have



where a white dot indicate no path crosses that portion of the boundary and a black dot indicates that a path does cross that portion of the boundary. The labels x_i indicate the weight for the particular vertex; here we choose the weights so that they are the same in each row of the domain.

Let v be a vertex and $w(v)$ be the weight of the vertex. For a path configuration \mathcal{C} that satisfies the boundary conditions we define the weight of the configuration $w(\mathcal{C})$ to be the product of the weights of each vertex. In our example, a valid configuration and its weight are



where we add a label of x_i on the left to indicate the weight parameter in each row.

The *partition function* is the sum of the weight of all the configurations obeying the boundary conditions:

$$Z = \sum_{\mathcal{C}} w(\mathcal{C}).$$

We stress that it will depend on the choice of boundary condition and that it is a function of the weights. In our example, we have

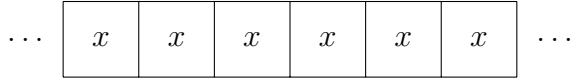
$$\begin{aligned} Z = & x_1^2 x_2 x_3 + x_1^2 x_2 x_4 + x_1^2 x_3 x_4 + x_1 x_2^2 x_3 + x_1 x_2^2 x_4 + 3x_1 x_2 x_3 x_4 + x_1 x_2 x_3^2 + x_1 x_3^2 x_4 \\ & + x_1 x_2 x_4^2 + x_1 x_3 x_4^2 + x_2^2 x_3 x_4 + x_2 x_3^2 x_4 + x_2 x_3 x_4^2 \end{aligned}$$

Note that if $w(\mathcal{C}) \geq 0$ for all configurations \mathcal{C} then we can define a probability distribution on the set of configurations by

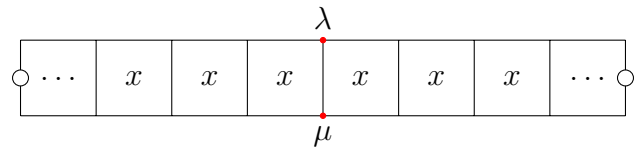
$$\mathbb{P}(\mathcal{C}) = \frac{w(\mathcal{C})}{Z}.$$

This is known as the *Gibbs measure* of the model in statistical physics, although here we won't touch much on the probabilistic aspects of the vertex models.

Let us relate this five vertex model back to our interlacing partitions. Suppose we have a single bi-infinite row of our vertex model



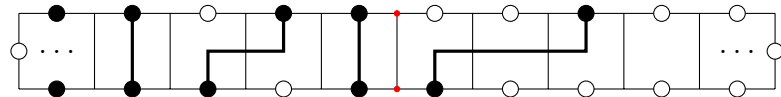
We need to give it boundary conditions and for that we return to Maya diagrams. First choose a location in our row to be the center and let μ and λ be partitions. To the bottom boundary assign boundary conditions corresponding to μ , that is, the center of the Maya diagram aligns with the center of the row and there is a path entering from the bottom if and only if there is a particle in the Maya diagram of μ . To the top assign boundary condition corresponding to λ . For the left and right boundaries (off at $\pm\infty$) we choose to have no paths entering or exiting. We draw the row with these boundary conditions as



where we use red dots to mark the center. We have the following Lemma.

Lemma 4.1. *If $\mu \preceq \lambda$ then there is a unique way to fill in the row with paths and it has weight $x^{|\lambda|-|\mu|}$. Otherwise, there is no valid way to fill in the row with paths and the weight is zero.*

Example 4.2. Let $\mu = (1, 1)$ and $\lambda = (3, 1, 1)$. Then the row with bottom boundary condition μ and top boundary condition λ (with no paths entering or exiting on the sides) has a unique valid path configuration given by



The weight of this configuration is $x^{|\lambda|-|\mu|} = x^3$. The red dots marks the center of the Maya diagrams which we also use to define the center of our row. Note that the row extends infinitely to the left with path that are vertical, and infinitely to the right with empty vertices.

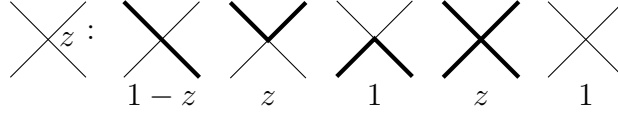
If the fact that the row is infinitely long bothers you, recall that for the Maya diagrams there is only a finite interval in which “interesting” things are happening. For fixed λ and μ we can always choose to have a finite but large enough row which captures all of this behavior. In the above example, it is enough to only keep the six center columns.

Exercise 17. Draw some examples of rows with boundary conditions given by a pair of partitions λ and μ , and compute the weight of the configurations. (Difficulty rating: 1)

Exercise 18. Prove Lemma 4.1. (Difficulty rating: 2)

4.2. Yang-Baxter Integrability. One of the main benefits of working with the vertex model is it provides extra local structure. In particular, our vertex model is *Yang-Baxter integrable*, a notion we will now describe.

Introduce a new set of vertices we'll call *crosses* such that the allowed local configurations are



where below we also write the corresponding weight.

These crosses and our original vertices satisfy the following relation

$$\begin{array}{c} j_3 \\ \square \\ y \\ x \\ \square \\ j_1 \end{array} = \begin{array}{c} j_3 \\ \square \\ x \\ y \\ \square \\ i_3 \end{array} \quad (4.1)$$

$$\begin{array}{c} i_1 \\ i_2 \\ \times \\ \square \\ y \\ x \\ \square \\ j_1 \\ j_2 \end{array} \quad \quad \quad \begin{array}{c} i_1 \\ i_2 \\ \square \\ y \\ x \\ \times \\ \square \\ j_1 \\ j_2 \end{array}$$

for any choice of $i_1, i_{2,3}, j_1, j_2, j_3 \in \{0, 1\}$, where these indicate a choice of fixed boundary condition both sides (with 0 indicating there is no path, and 1 indicating there is a path), x and y are the weight parameters at each vertex, and we sum the weights over all possible interior path configurations on both side. In other words, if we fix the same boundary condition on both sides, then the partition functions are equal. This is known as the *Yang-Baxter equation*. We'll abbreviate it as the YBE.

Note that we move the cross from the left to the right of vertices and the vertices swap: on the left side the bottom comes with the parameter x and the top comes with parameter y , on the right side it is swapped.

Example 4.3. Suppose we set $i_1 = j_2 = 1$ and the rest to zero. Then the YBE says we have the following equality of partition functions:

$$\begin{array}{c} \bullet \\ \circ \\ \times \\ \square \\ y \\ x \\ \square \\ \circ \\ \bullet \end{array} = \begin{array}{c} \bullet \\ \circ \\ \square \\ y \\ x \\ \square \\ \circ \\ \bullet \end{array}$$

Explicitly writing the sum over path configurations, this becomes

$$w \left(\begin{array}{c} \bullet \\ \circ \\ \times \\ \square \\ \square \\ \square \\ \square \\ \circ \\ \bullet \end{array} \right) + w \left(\begin{array}{c} \bullet \\ \circ \\ \times \\ \square \\ \square \\ \square \\ \square \\ \circ \\ \bullet \end{array} \right) = w \left(\begin{array}{c} \bullet \\ \circ \\ \square \\ y \\ x \\ \square \\ \circ \\ \bullet \end{array} \right)$$

where we see there are two ways to fill in the paths on the left but only one on the right. Computing the weights we have

$$\text{LHS: } \left(1 - \frac{y}{x}\right) \cdot y + \frac{y}{x} \cdot y = y$$

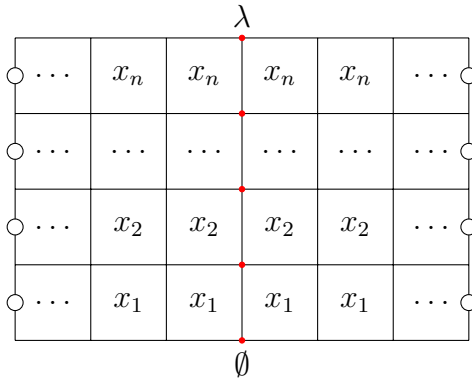
$$\text{RHS: } x \cdot \frac{y}{x} = y$$

which are in fact equal.

As there are only $2^6 = 64$ choices of boundary conditions, there are only 64 equations needed to be checked to see that the YBE holds. In principle, this could be checked by hand. Generally, however, the YBE follows from the representation theoretic origins of our vertex model, in particular the fact that they are related to so-called R matrices of quantum groups.

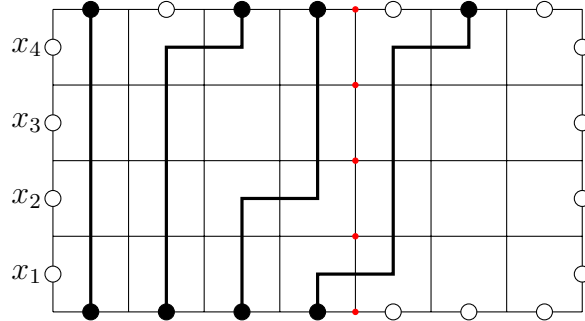
To see an example of what we can get from the YBE, let's return to the case of semi-standard Young tableaux. We begin with a proposition whose proof we leave as an exercise.

Proposition 4.4. *There is a bijection between semi-standard Young tableaux of shape λ with maximum filling n and 5-vertex path configurations on the domain*



Moreover, the partition function of the vertex model is exactly the Schur polynomial $s_\lambda(x_1, \dots, x_n)$.

Example 4.5. Let $\lambda = (2, 1, 1)$ and let the maximum filling be $n = 4$. Then one possible path configuration of the above domain is



where it extends to the left with vertical paths and to the right with empty space. This corresponds to the semi-standard Young tableaux

1	4
2	
4	

We can read off the sequence of interlacing partitions from the vertex model by looking at the positions the paths exit the top of each row. In this example, we have

$$\emptyset \preceq (1) \preceq (1, 1) \preceq (1, 1) \preceq (2, 1, 1)$$

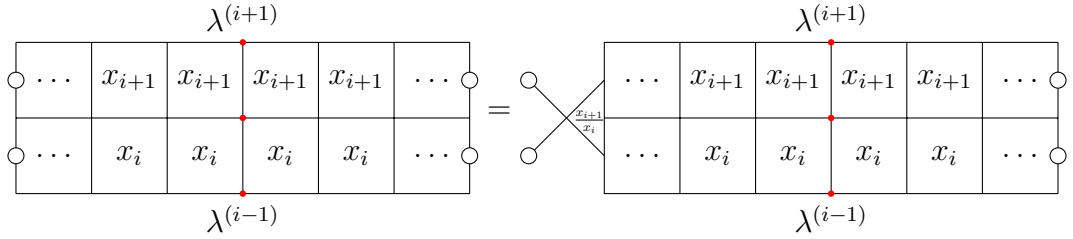
We'll now use the YBE to prove that Schur polynomials are symmetric, that is for any permutation $\sigma \in S_n$ we have

$$s_\lambda(x_1, x_2, \dots, x_n) = s_\lambda(x_{\sigma(1)}, x_{\sigma(2)}, \dots, x_{\sigma(n)}).$$

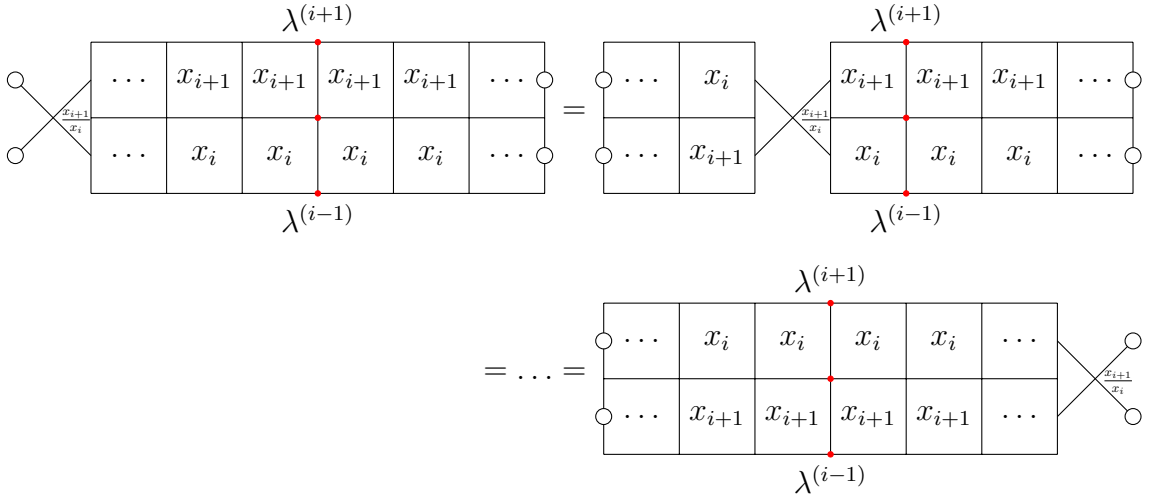
Since any permutation can be built from transpositions of the form $(x_i, x_{i+1}) \mapsto (x_{i+1}, x_i)$, it is enough to show

$$s_\lambda(x_1, \dots, x_i, x_{i+1}, \dots, x_n) = s_\lambda(x_1, \dots, x_{i+1}, x_i, \dots, x_n).$$

To that end let's look at the i -th and $(i+1)$ -st row of our vertex model. We can insert a cross at the far left and get



as with these boundary conditions the cross can only be empty and contributes a weight of 1. Now repeatedly using the YBE, we have



We are able to swap the rows! We can remove the cross at the right end as it again must be empty and so it contributes a weight of 1. This process of pushing a cross across a pair of rows in order to swap them is sometimes referred to as the “train argument.”

Altogether, we have shown we have the equality of partition functions

$$\begin{array}{c}
 \text{Diagram showing two Young diagrams labeled } \lambda \text{ connected by an equals sign.} \\
 \text{The left diagram has columns labeled } \dots, x_n, x_n, x_n, x_n, \dots. \\
 \text{The right diagram has columns labeled } \dots, x_n, x_n, x_n, x_n, \dots. \\
 \text{Both diagrams have rows labeled } \emptyset \text{ at the bottom.}
 \end{array}$$

By Proposition 4.4, the partition function on the LHS is $s_\lambda(x_1, \dots, x_i, x_{i+1}, \dots, x_n)$ and the one on the RHS is $s_\lambda(x_1, \dots, x_{i+1}, x_i, \dots, x_n)$. It follows that the Schur polynomials are symmetric.

Exercise 19. Prove Proposition 4.4. (Difficulty rating: 2)

4.3. The second five-vertex model. We will need a second five vertex model. We will draw the vertices in gray to distinguish them from the previous vertex model. The five possible vertices and their weights are draw below:

$$\begin{array}{c}
 \text{Diagram showing five possible vertex configurations:} \\
 \text{1. A single gray square labeled } x. \\
 \text{2. A gray square with a small white rectangle at the bottom-right corner labeled } x. \\
 \text{3. A gray square with a small white rectangle at the top-right corner labeled } 1. \\
 \text{4. A gray square with a horizontal white bar in the middle labeled } 1. \\
 \text{5. A gray square with a vertical white bar in the middle labeled } x. \\
 \text{6. A gray square with a small white rectangle at the top-left corner labeled } x.
 \end{array}$$

Note that the possible path configurations are the same, it is only the weights that have changed. In fact, if $w_x(v)$ is the weight of a vertex in the first vertex model, the corresponding weight in this new vertex model is $x \cdot w_{1/x}(v)$.

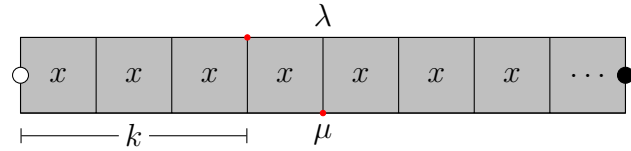
Since this vertex model differs from the previous vertex model only through a change of variable in the weight, the YBE still holds. In particular, we have

$$\begin{array}{ccc}
 \text{Diagram showing the Yang-Baxter equation for the second five-vertex model.} \\
 \text{Left side:} & \text{Right side:} & \\
 \text{A central gray square with boundary labels } j_3 \text{ (top), } i_1 \text{ (left), } i_2 \text{ (bottom-left), } yx \text{ (bottom-right), } j_2 \text{ (right).} & = & \text{A central gray square with boundary labels } j_3 \text{ (top), } i_1 \text{ (left), } i_2 \text{ (bottom-left), } yx \text{ (bottom-right), } j_2 \text{ (right).} \\
 \text{Below the central square are boundary labels } j_1 \text{ and } i_3. & & \text{Below the central square are boundary labels } j_1 \text{ and } i_3.
 \end{array}$$

for any choice of boundary condition $i_1, i_2, i_3, j_1, j_2, j_3 \in \{0, 1\}$.

As you might expect, this vertex model can also be related to our interlacing partitions. The following lemma describes this relationship.

Lemma 4.6. Let λ and μ be partitions, and k an integer such that $\lambda_i = \mu_i = 0$ for all $i \geq k$. Consider the semi-infinite row with boundary condition shown below:



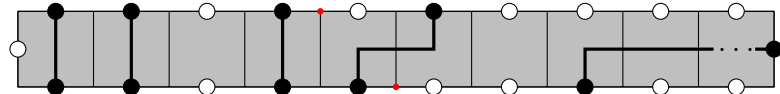
There is a unique valid path configuration for this row if and only if $\mu \succeq \lambda$. It has weight $x^k x^{|\mu|-|\lambda|}$. Otherwise, there is no valid path configurations and the weight is zero.

Notice the differences here compared to the previous vertex model:

- The partition on the bottom boundary is now larger, i.e. $\mu \supset \lambda$.
- We center the Maya diagram on top one column to the left of the one on the bottom.
- On the right boundary our boundary condition has a path exiting.
- The row is no longer infinite to the left.

The last condition is necessary since in the gray vertex model vertical paths come with a weight of x , so if the row extended infinitely to the left we would have an infinite power in our weight.

Example 4.7. Let $\mu = (3, 1, 1)$, $\lambda = (2, 1)$, and $k = 4$. Then the row with bottom boundary condition μ and top boundary condition λ has a unique valid path configuration given by

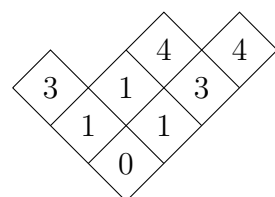


The weight of this configuration is $x^k x^{|\mu|-|\lambda|} = x^{4+2} = x^6$. Note that the $x^{|\mu|-|\lambda|} = x^2$ comes from the empty vertices, while the $x^k = x^4$ comes from the number of paths exiting at the top.

Exercise 20. Prove Lemma 4.6. This is less straight forward than Lemma 4.1. The comments at the end of Example 4.7 may be helpful. (Difficulty rating: 2)

5. REVERSE PLANE PARTITIONS REVISITED

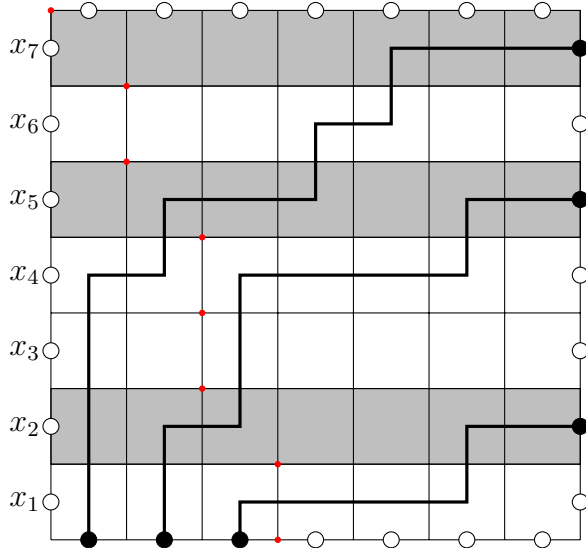
In this section we will use the extra structure provided by the vertex models in order to prove Theorem 3.6. It will be easiest to see in terms of a specific example, so let us return the Example 3.8 of a reverse plane partition of shape $\lambda = (4, 3, 1)$.



By Theorem 3.9 a reverse plane partition can be mapped to a sequence of interlacing partitions. In this case, we have

$$\emptyset \preceq (3) \succeq (1) \preceq (1, 0) \preceq (4, 1) \succeq (3) \preceq (4) \succeq \emptyset$$

Now, using Lemmas 4.1 and 4.6, we can map this to a path configuration using our vertex model. Whenever we see a \preceq we will have a row of white vertices, while whenever we see a \succeq we put a gray row. The specific partitions tell us at what positions the paths cross between the rows. In our example, we have



Note the number of paths is the number of non-zero parts of λ . We could include some number of zero parts in λ which would result in extending our domain to the left with columns containing vertical paths. But this is unnecessary.

One can check that the above gives a bijection between reverse plane partitions of shape λ and path configuration of a certain vertex model in which the type of rows depend on λ . However, we have not mentioned what weights we should choose for our vertices. We would like to pick them so that the total weight of the path configuration is equal to q to the volume of the reverse plane partition.

Lemma 5.1. *Let Λ be a reverse plane partition and $\ell(\lambda)$ be the number of non-zero parts of λ . Let \mathcal{C} be the corresponding path configuration under the bijection described above. Then if one chooses the parameters of the vertex model to be $x_i = q^{\pm i}$ where we take + for a gray row and - for a white row, we have*

$$q^{vol(\Lambda)} \cdot A_\lambda(q) = w(\mathcal{C})$$

where $A_\lambda(q) = q^{\sum_{i=1}^{\ell(\lambda)} (\lambda_i - i + \ell(\lambda))(i-1)}$ is completely determined by the shape λ and is independent of the specific configuration.

Proof. Suppose that the sequence of interlacing partitions corresponding to our reverse plane partition Λ are given by

$$\emptyset = \lambda^{(0)}, \lambda^{(1)}, \lambda^{(2)}, \dots, \lambda^{(n)}, \lambda^{(n+1)} = \emptyset$$

where $n = h_\lambda((1, 1))$. Note that we can write the volume of the reverse plane partition as

$$vol(\Lambda) = |\lambda^{(1)}| + |\lambda^{(2)}| + \dots + |\lambda^{(n)}|$$

Let's look at rows i and $i+1$, $i = 1, \dots, n$ of the vertex model. Note the bottom boundary of this pair of rows is given by $\lambda^{(i-1)}$, the top boundary is given by $\lambda^{(i+1)}$, and in between we have $\lambda^{(i)}$. Note that these are the only rows where the weight will depend explicitly on $\lambda^{(i)}$. There are four case for the types of rows. Let's look at the weight of the rows in each of these cases.

- $\lambda^{(i-1)} \preceq \lambda^{(i)} \preceq \lambda^{(i+1)}$: This means we have two white rows. The weight is given by

$$x_i^{|\lambda^{(i)}| - |\lambda^{(i-1)}|} x_{i+1}^{|\lambda^{(i+1)}| - |\lambda^{(i)}|}.$$

Looking only at the parts involving $\lambda^{(i)}$, we see that we would like

$$(x_i x_{i+1}^{-1})^{|\lambda^{(1)}|} = q^{|\lambda^{(i)}|} \iff x_i x_{i+1}^{-1} = q$$

Choosing $x_i = q^{-i}$ and $x_{i+1} = q^{-(i+1)}$ gives the desired equality.

- $\lambda^{(i-1)} \preceq \lambda^{(i)} \succeq \lambda^{(i+1)}$: This means row i is white, while row $i+1$ is gray. The weight of the two rows is

$$x_i^{|\lambda^{(i)}| - |\lambda^{(i-1)}|} x_{i+1}^{k_{i+1}} x_{i+1}^{|\lambda^{(i)}| - |\lambda^{(i+1)}|}$$

where k_{i+1} is the number of paths exiting row $i+1$. Looking only at the parts involving $\lambda^{(i)}$, we see that we would like

$$(x_i x_{i+1})^{|\lambda^{(1)}|} = q^{|\lambda^{(i)}|} \iff x_i x_{i+1} = q$$

Choosing $x_i = q^{-i}$ and $x_{i+1} = q^{i+1}$ gives the desired equality.

- $\lambda^{(i-1)} \succeq \lambda^{(i)} \preceq \lambda^{(i+1)}$: This means row i is gray, while row $i+1$ is white. The weight of the two rows is

$$x_i^{k_i} x_i^{|\lambda^{(i-1)}| - |\lambda^{(i)}|} x_{i+1}^{|\lambda^{(i+1)}| - |\lambda^{(i)}|}$$

where k_i is the number of paths exiting row i . Looking only at the parts involving $\lambda^{(i)}$, we see that we would like

$$(x_i x_{i+1})^{-|\lambda^{(1)}|} = q^{|\lambda^{(i)}|} \iff x_i^{-1} x_{i+1}^{-1} = q$$

Choosing $x_i = q^i$ and $x_{i+1} = q^{-(i+1)}$ gives the desired equality.

- $\lambda^{(i-1)} \succeq \lambda^{(i)} \succeq \lambda^{(i+1)}$: This means both rows are gray. The weight of the two rows is

$$x_i^{k_i} x_i^{|\lambda^{(i-1)}| - |\lambda^{(i)}|} x_{i+1}^{k_{i+1}} x_{i+1}^{|\lambda^{(i)}| - |\lambda^{(i+1)}|}$$

Looking only at the parts involving $\lambda^{(i)}$, we see that we would like

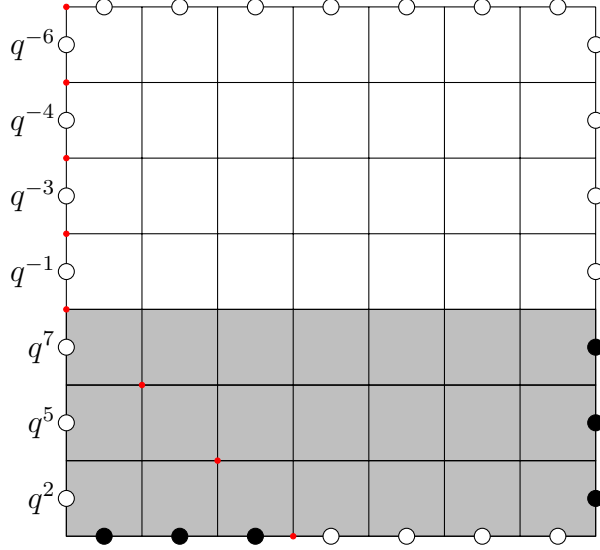
$$(x_i^{-1} x_{i+1})^{|\lambda^{(1)}|} = q^{|\lambda^{(i)}|} \iff x_i^{-1} x_{i+1} = q$$

Choosing $x_i = q^i$ and $x_{i+1} = q^{i+1}$ gives the desired equality.

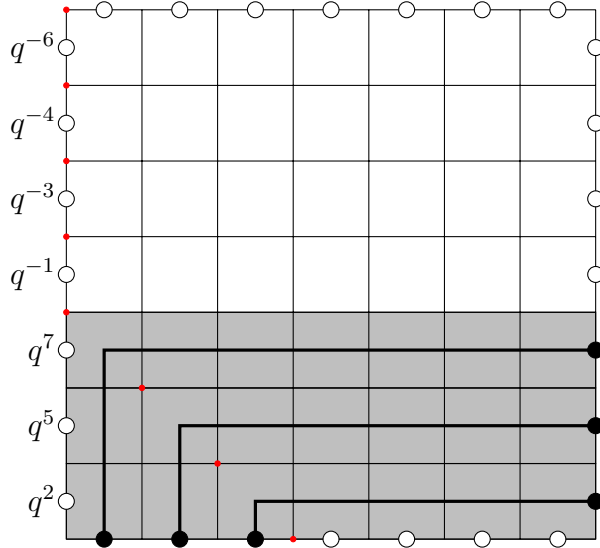
We see that choosing $x_i = q^{\pm i}$ with $+$ for gray and $-$ for white makes the weight of the path configuration proportional to $q^{vol(\Lambda)}$. However, we have extra $x_i^{k_i}$ factors whenever row i is a gray row. These combine to give the extra factor of $A_\lambda(q)$. \square

This lemma, along with the bijection between reverse plane partitions and path configurations, tells us that up to an overall factor the generating function of reverse plane partitions of shape λ is equal to the partition function Z_λ of a certain vertex model. We are left to compute this partition function. For this we rely on the YBE (4.1). Let's see how this works in our example.

In our running example, we have three gray rows and four white rows. Let's consider a vertex model with all the gray rows on the bottom and all the white rows on top.



After some inspection, you can notice that there is only one valid path configuration for this vertex model

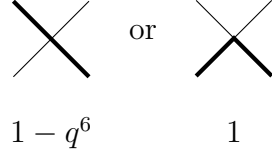


and it has weight $A_\lambda(q)$. Now we would like to rearrange the rows into the vertex model from our example. To do this we turn to the YBE.

Let's look at rows three and four. We can use the train argument to get

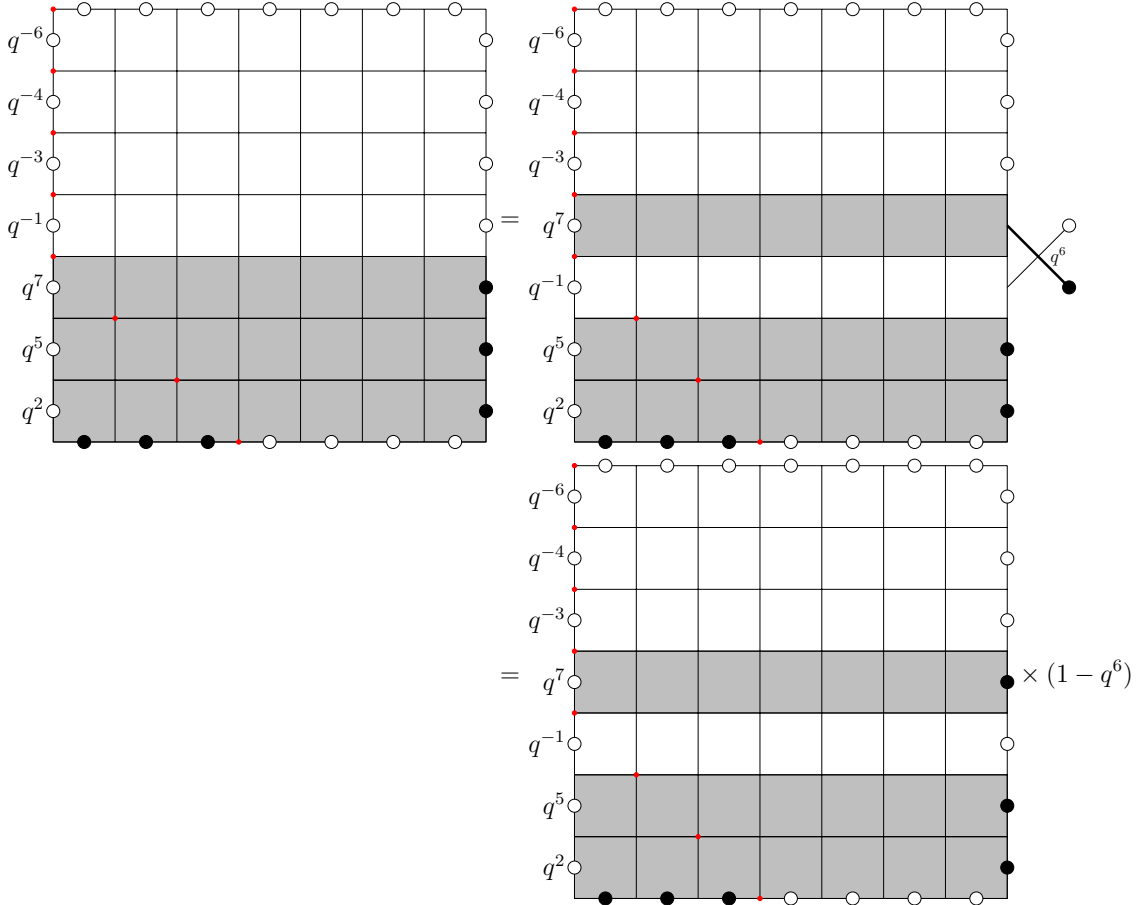
$$\begin{array}{c}
 \text{Diagram showing the Yang-Baxter equation (YBE) for rows 3 and 4. It consists of two boxes of 8x8 grids. The top-left box has a crossing with factor } q^5. \text{ The bottom-right box has a crossing with factor } q^6. \\
 = \begin{array}{c} \text{Diagram showing the Yang-Baxter equation (YBE) for rows 3 and 4. It consists of two boxes of 8x8 grids. The top-left box has a crossing with factor } q^7. \text{ The bottom-right box has a crossing with factor } q^6. \\ = \dots = \begin{array}{c} \text{Diagram showing the Yang-Baxter equation (YBE) for rows 3 and 4. It consists of two boxes of 8x8 grids. The top-left box has a crossing with factor } q^7. \text{ The bottom-right box has a crossing with factor } q^6. \end{array} \end{array}
 \end{array}$$

We would like to remove the cross at right side. There are two options for how the path look in the cross:



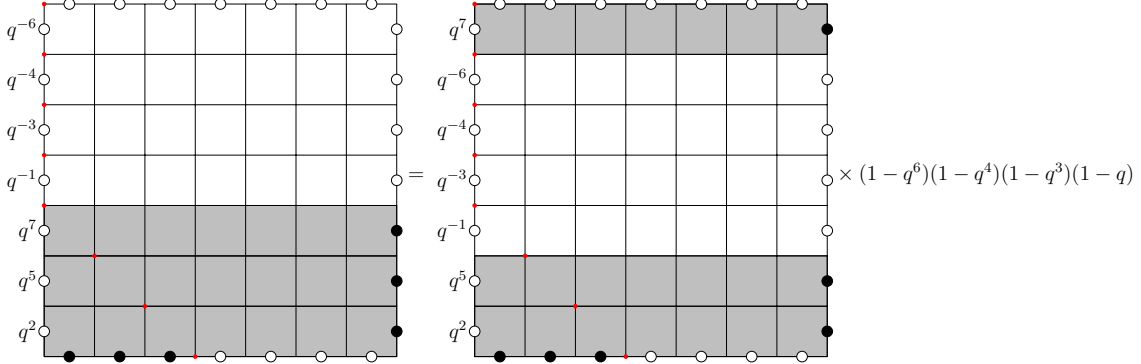
If we choose the right option then the path must exit to the right in the white row. There will be an infinitely long segment of vertices in which in the bottom row there is a path going horizontal while the top row is empty. Each of these pairs contributes a weight of q^6 . If we choose q such that $|q| < 1$, then the infinite power of q will give the rows zero weight.

If we choose the left option then we have a finite power of q in the weight, so the weight stays nonzero. Thus we have



where we remove the cross on the right at the cost of its weight $1 - q^6$. We can repeat this process, moving the top gray row all the way to the top collecting the

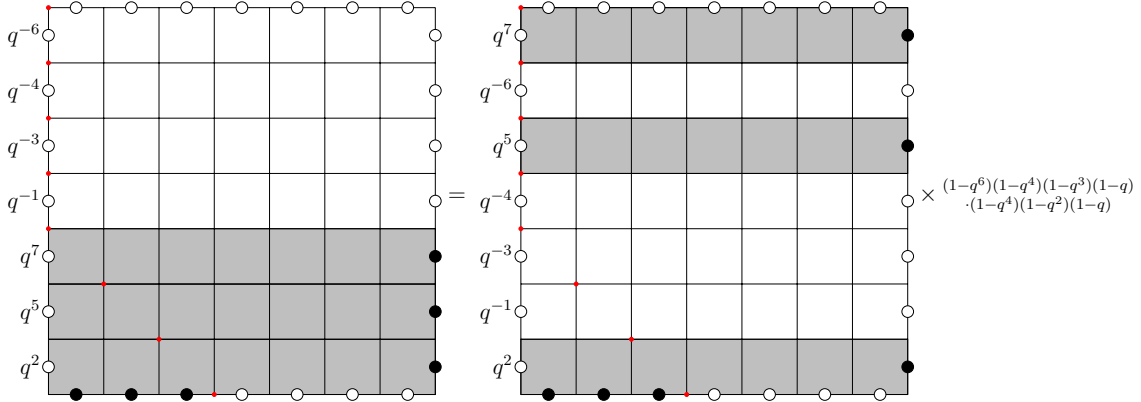
weight of the crosses along the way. We get



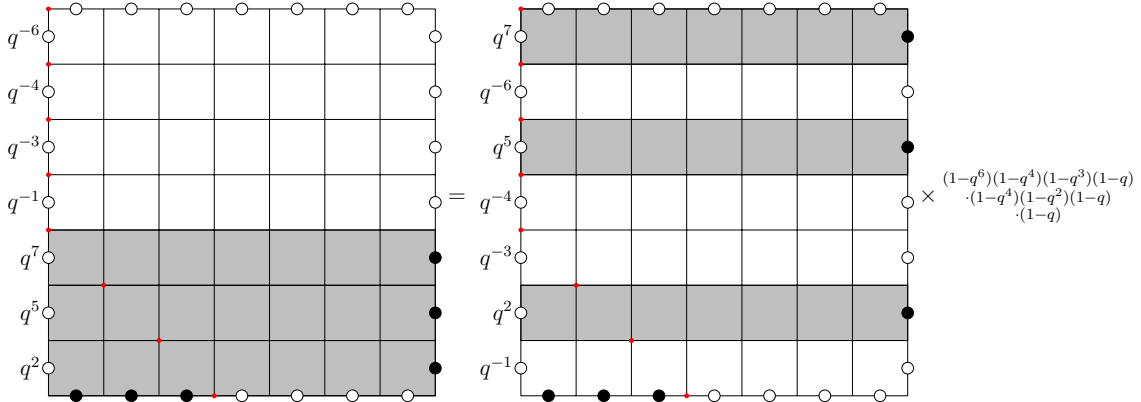
Notice that the powers of q here are exactly the hook length of the first row of λ :

$$(1-q^6)(1-q^4)(1-q^3)(1-q) = \prod_{x \in \text{first row of } \lambda} (1-q^{h_\lambda(x)})$$

We now move the next gray row to the correct position



where the new factors of q are the hook length of the second row of λ . Now the final gray row:



We can divide the terms on the RHS coming from the crosses onto the LHS and we get

$$Z_\lambda = A_\lambda(q) \prod_{x \in \lambda} \frac{1}{1 - q^{h_\lambda(x)}}.$$

Recall from Lemma 5.1 that we have

$$Z_\lambda = A_\lambda(q) \sum_{\Lambda \in RPP(\lambda)} q^{vol(\Lambda)}.$$

Putting these together, we see that

$$\sum_{\Lambda \in RPP(\lambda)} q^{vol(\Lambda)} = \prod_{x \in \lambda} \frac{1}{1 - q^{h_\lambda(x)}}$$

as desired.

Exercise 21. Show that this works in general, thus proving Thm. 3.6. (Difficulty rating: 3)

6. A LITTLE BIT EXTRA

Note that the we by choosing a rectangular partition, the generating function for RPP given in Thm. 3.6 implies the generating function for PP with restricted numbers of rows and columns given in Prop. 3.3. (See Exercise 15.) However, in the world of plane partitions often more restrictions are added. For example, one often considers plane partitions with restrictions on the number of columns, the number of rows, and the maximum allowed filling. These are called *boxed plane partitions*. Suppose the number of rows is restricted to be a , number of columns restricted to be b , the maximum filling restricted to be c . In terms of stacks, of cubes, one can think of the stacks being restricted to stay inside an $a \times b \times c$ box (thus the name). In terms of lozenge tilings, these correspond to tilings of an $a \times b \times c$ hexagon.

Boxed plane partitions also have a nice generating function. Let $\mathcal{B}(a, b, c)$ denote the set of all boxed PP described above. We have

Theorem 6.1. *The generating function for plane partitions restricted to an $a \times b \times c$ box is given by*

$$\sum_{\Lambda \in \mathcal{B}(a, b, c)} q^{|\Lambda|} = \prod_{i=1}^a \prod_{j=1}^b \prod_{k=1}^c \frac{1 - q^{i+j+k-1}}{1 - q^{i+j+k-2}} = \prod_{i=1}^a \prod_{j=1}^b \frac{1 - q^{i+j+c-1}}{1 - q^{i+j-1}}.$$

Since we are restricting everything to fit in an $a \times b \times c$ box, there are a finite number of possible plane partitions (this is not this case if the maximum allowed filling is unrestricted). By carefully taking the limit as $q \rightarrow 1$ in the above theorem, we have

Corollary 6.2. *Let $N(a, b, c)$ be the number of plane partitions restricted to an $a \times b \times c$ box. Then*

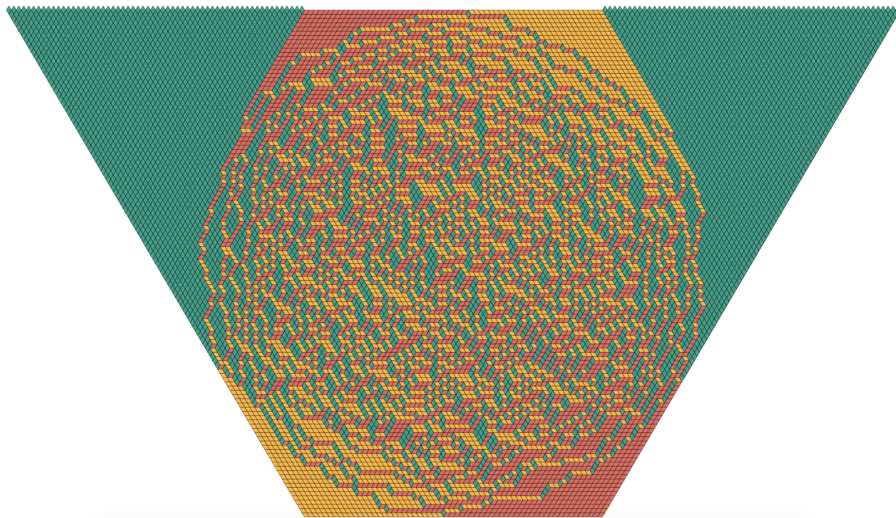
$$N(a, b, c) = \prod_{i=1}^a \prod_{j=1}^b \prod_{k=1}^c \frac{i + j + k - 1}{i + j + k - 2}.$$

(Equivalently, this counts the number of lozenge tilings of an $a \times b \times c$ hexagon.)

Exercise 22. Prove Cor. 6.2 starting from Thm. 6.1. (Difficulty rating: 2)

One might try to prove Thm. 6.1 via the vertex model just as we did for Thm. 3.6. The extra restriction on the maximum allowed filling translates to a restriction on the length of the rows of the vertex model. Unfortunately, this makes our row swapping argument using the YBE more difficult (can you see why this is the case?) and I am not aware of a way to make the argument work.

For some final remarks, I'd like to mention that there is a large field of study involving large random tilings. As we have seen lozenge tilings are related to plane partitions, and there are many other cases where tilings can be translated to other combinatorial objects. Understanding the combinatorics can help understand certain probabilistic questions. I leave you with a lozenge tiling of a $120 \times 120 \times 120$ hexagon chosen uniformly at random from all possible lozenge tiling (ignore the top left and top right corners which are frozen due to the boundary conditions on the top).



(Courtesy of Leo Petrov: <https://lpetrov.cc/>)